# Low Energy Neutral Atoms Observed near the Earth

G. R. Wilson

Mission Research Corporation, Nashua NH

T. E. Moore and M. Collier

Goddard Space Flight Center, Greenbelt MD

**Abstract**

During the summer of 2000 the LENA instrument on the IMAGE spacecraft collected a unique data set of low energy, neutral atom emissions. The data suggests an ever present flux of low energy (< 50 eV) oxygen neutrals in the near earth environment, typically below 4000 km altitude. Because of two different patterns in the images made during a number of spacecraft perigee passes we infer at least two main sources for these particles. One (possibly from the auroral zone) produces a high degree of variability from one image to the next and creates more energetic particles, and another (possibly part of the hot oxygen geocorona) gives less variability within a sequence of images and lower energy particles. Overall, the measured neutral fluxes increase with increasing magnetic activity. During southern-hemisphere winter the total neutral flux rates vary diurnally with peak intensity near 0740 UT and a minimum near 1940 UT. Near perigee neutral fluxes are often seen coming from a broad range of directions so that a localized source, such as the auroral zone, alone can't produce it. Processes affecting low energy oxygen neutrals, such as gravitational deflection or spacecraft ram deflection, cannot broaden a localized source enough to match the data.

## Introduction

It has been recognized for about 20 years now that energetic neutral atoms (ENA), produced when near earth plasma populations exchange charge with gases in the earth's geocorona, can be used to remotely probe the plasmas which produce them [*Roelof*, 1987]. Much of the early work with this technique used data from instruments not primarily designed for ENA imaging [*Henderson et al.*, 1997] but was still able to deduce important properties of the ring current and injected plasma populations [*Reeves and Henderson*, 2001; *Jorgensen et al*., 2001]. The desire to more fully exploit this diagnostic tool was one of the main motivations for the IMAGE mission, which carried three neutral atom instruments into orbit.

Prior to the initial planning stages for the IMAGE mission it was realized that relatively low energy (< 1 keV) neutrals could be detected and imaged by charge conversion on reflection from a crystalline surface [*Herrero and Smith*, 1992]. This concept is the basis of the Low Energy Neutral Atom (LENA) instrument on IMAGE [*Moore et al.*, 2000] which can detect neutrals at energies down to about 10 eV. One of the motivations for LENA was the desire to study ion energization in the auroral zone where ionospheric ions are routinely energized to the 10-1000 eV range. With the large ion fluxes and high neutral densities (particularly atomic oxygen) in this region it was thought that it should be a copious producer of ENA in this energy range. Early results from the LENA instrument have confirmed this idea [*Moore et al.*, 2001].

The LENA instrument was not the first to observe relatively low energy neutrals coming from the high latitude ionosphere. The PIPPI (Prelude In Planetary Particle Imaging) instrument on the Swedish microsatellite Astrid [*C:son Brandt et al*., 2001] was able to detect neutrals in the ~0.1-10 keV range, coming from the polar cap below the satellites orbital altitude of 1000 km. Fluxes of $10^6$ $(cm^2\ sr\ s)^{-1}$ were seen coming from an arc like region in the 70˚ - 85˚ magnetic latitude range that extended from dusk through nightside local times. This emission pattern is in approximate agreement with what is expected from a low altitude (≤ 400 km) source region where the ion velocity distribution is highly peaked in a direction perpendicular to the local magnetic field [*C:son Brandt et al*. 2000].

One plasma populations that could give rise to the neutral fluxes seen by PIPPI and LENA are ionospheric $O^+$ and $H^+$ ions energized in or near the auroral zone. These have been the subject of intense study over the last thirty years where it has been demonstrated that large fluxes of ions with escape energy come from several source regions and are energized by multiple mechanisms operating over a range of altitudes [*Yau and André*, 1997; *André and Yau*, 1997]. The energization starts at very low altitudes (<1000 km) as has been demonstrated by sounding rocket observations [*Lynch et al.*, 1996]. Statistical analysis of large quantities of satellite ion data has shown the seasonal, magnetic and solar activity dependence of the outflow fluxes [*Yau et al.*, 1985].

The purpose of this paper is to examine in detail the neutral fluxes measured by the LENA instrument when the IMAGE spacecraft passed through perigee. This perigee pass data contain some of the most intense fluxes seen by the LENA instrument in broad diffuse patterns that appear to have a ram component.

## Instrument Description

The LENA instrument was carried into orbit on the IMAGE spacecraft, launch on 25 March 2000. The orbit for the spacecraft is elliptical with an apogee altitude of 7 $R_E$ and a perigee altitude of 1000 km. Its orbital period is about 14.2 hours, so that IMAGE makes at most two perigee passes per day. At the beginning of the time interval of interest to this paper (10 June 2000) the IMAGE orbit plane was close to the dawn-dusk meridian. Near the end of the interval (29 August 2000) this plane had rotated to near the noon-midnight meridian.

The LENA instrument is designed to image low energy neutral atoms (10-300 eV). It has a fan shaped field-of-view that is $90^\circ \times 8^\circ$ that is divided into 12, $7.5^\circ \times 8^\circ$ pixels. A full image ($360^\circ \times 90^\circ$) is built up over one spin period of the spacecraft (~2 min). Neutrals, ions and photons enter the front slit of the instrument passing through a series of charged collimator plates designed to remove most of the charge particles entering the instrument. For the data discussed in this paper the collimator potential was set at 8.8 kV which is sufficient to filter out ions with energies up to ~50 keV/e. Photons might produce a response in the instrument by either reflecting off of multiple surfaces to a microchannel plate, or by ionizing some of the residual gas in the instrument. *Collier et al.* [2001] demonstrates quite nicely that neither of these two processes is significance, even when viewing direct sun light.

A fraction of the neutrals that enter the instrument and reflect off of the conversion surface leave that surface as a negative ion. These ions are picked up by the extraction optics, accelerated to about 12 keV and then focused on a start foil, in one dimension according to initial energy and in the other dimension according to the polar angle of its entrance. Although the polar angle response of the instrument was tested before launch its in-orbit response differs from the calibration results so that we have been unable to flat field the images in the polar angle dimension. For this reason all data presented here will be integrated over the polar angle and only presented versus the spin angle. We know that the spin angle response of the instrument is reliable because the instrument puts the sun pulse and the interstellar neutral signals [Moore et al., 2002] in the right spin phase.

The probability that the tungsten conversion surface makes a negative ion out of an incident neutral increases with the energy of the neutral. As a result, the instrument's effective area increases with energy; as much as two orders of magnitude for oxygen between .02 and 1.0 keV (see figure 12 in *Moore et al.* [2000]). Of particular importance to the subject of this paper is the low energy cutoff of the instrument. For hydrogen there appears to be a steep drop-off in sensitivity between 10 and 20 eV. The lowest energy tested for oxygen neutrals was 30 eV with the response still following its normal trend. Somewhere below 30 eV there should be a similar sharp drop off in instrument response for oxygen but it is not known where that cutoff is.

Another conversion surface issue is the fact that incident neutrals can sputter negative ions of other species from the surface. Oxygen neutrals, with energies as low as 30 eV, can sputter significant quantities of $H^-$ ions but incident hydrogen neutrals only begin to sputter significant numbers of $O^-$ ions at energies above 300 eV. For this reason composition information cannot be taken at face value but must be examined carefully.

For a full description of the instrument see *Moore et al.* [2000].

**LENA Perigee Pass Data**

In this section we describe many of the basic aspect of the LENA data gathered during perigee passes of the IMAGE spacecraft between 10 June and 29 August 2000. During this time interval the spacecraft made about 137 perigee passes of which 104 have been analyzed. The remaining 33 have not been analyzed because of poor or missing data. Shortly after the 29$^{th}$ of August 2000 the instrument experienced a series of high voltage discharges. The resulting damage to the instrument plus subsequent changes made in the way the instrument was operated during perigee pass resulted in the loss of the perigee pass signal seen in the preceding three months.

The first example we show is the first perigee pass from 15 June 2000. At the beginning of this pass Kp was 6-, changing to 3-. Dst was –2 nT, i.e. no magnetic storm in progress. During the 30 minutes of the pass the Kyoto quick look AE index increased from about 250 nT to about 400 nT. In the two hours before the perigee pass the IMF was mostly northward and the solar wind dynamic pressure was constant at about 2 nPa.

Figure 1 shows a spin-time spectrogram summarizing this pass. Each vertical strip is a single image gathered over a two-minute spin of the spacecraft. The vertical axis indicates spin sector going from top to bottom in the order in which they were recorded. Lines on this figure indicate several important directions. The dotted line at spin sector 17 indicates when the instrument looks in the nadir direction. The dashed curve indicates when LENA was looking along the spacecraft velocity vector (Ram direction). The upper (lower) dashed dotted curve indicates the trailing (approaching) limb of the earth. Spin sectors marked with the diamonds indicate when the instrument was closest to looking at the sun. On this date the sun was not directly in the field of view of the instrument, however, a faint diffuse signal can be seen around the sun direction. Because of the scale used in figure 1 this "sun pulse" signal is not apparent and for most of the figure is overwhelmed by the main perigee signal.

Below the spin time spectrogram in figure 1 is a plot of the ratio of the number of oxygen to hydrogen neutrals detected for each image. This is found by dividing, for the image as a whole, the integrated number of time-of-flight events under the oxygen peak by those under the hydrogen peak, after correcting each for background events.

One can see in this figure that as the spacecraft approaches perigee the intensity of the images increases and counts are seen over a broader range of spin sectors. After perigee the process appears to reverse, but part of the outbound interval is obscured as the spacecraft passes through the radiation belts. IMAGE entered the radiation belts outbound at about 0322 UT on this date. At about 0311 UT the instrument executed a time tagged command to reduce the voltage on the stop mcp in order to reduce the sensitivity of the instrument prior to radiation belt passage. (The reduction in image intensity has been corrected in the spin-time spectrogram.) This is the cause of the reduction in the O/H ratio by a factor of 10. It is not known why this reduction occurs but it was observed in all of the 105 perigee passes where a similar mcp voltage drop took place. Another thing to note in this sequence of images is the shift in the spin sector peak of the emissions from near nadir toward the approaching limb. The peak appears to be tracking either the shifting direction to the sun or the shifting ram direction.

The next two example passes are from 5 July 2000. In terms of magnetic activity this was a quiet day. The Dst index indicated that no magnetic storm was in progress. At the time of the earlier pass Kp was 2+ and for the later pass it was 1-. In the two hours before the first pass the IMF was southward with a magnitude of 5 nT and the solar wind dynamic pressure was constant at about 2 nT. The Kyoto quick look AE index was increasing from about 400 to 500 nT at the time. Four the two hours before the second perigee pass the IMF was mostly northward at about 6 nT with a constant dynamic pressure of 2 nPa. The Kyoto quick look AE index was steady and less than 100 nT.

Figures 2 and 3 show the summary data from these passes. The format for these figures is the same as figure 1. The only reference line to change in these figures, relative to figure 1, is the sun direction that has shifted lower in the spectrogram as the spacecraft orbit plane precesses. Trends similar to those from figure 1 are apparent here as well. In figure 2 the stop mcp voltage reduction took effect midway through the image that starts at 0706:38 UT.

Figure 3 illustrates a feature that occurs in a significant number of the perigee passes. That is the dramatic increase in intensity from one image to the next that occurs at 2113:37 UT. This change in intensity cannot be accounted for by any change in the state of the instrument.

In comparing the two passes from July $5^{th}$ one can easily see that the pass from later in the day is, overall, much dimmer than the earlier pass. In this data set it is very common to observe back to back perigee passes where the one occurring later in the day is the dimmer of the two. Because of the higher level of magnetic activity for the first pass compared to the second, some of the difference may be due to different rates of auroral zone ion energization. More will be said about this effect later.

Our last example, shown in figure 4, is for a very quiet interval on 24 August 2000. (Dst = -3 nT; Kp = 1+; Kyoto quick look AE < 50 nT; IMF northward ~10 nT; dynamic pressure constant ~1.5 nPa). There is no significant reduction in the O/H ratio for this pass because a stop mcp voltage drop, comparable to those which occurred in the previous passes, did not occur. On July 31, 2000 the software controlling the operation of the instrument was changed. After that date, instead of executing a time tagged command to turn down the stop mcp voltage the instrument used detected counts as a guide for when to make the reduction. As a result LENA tended to remain at a higher level of sensitivity through out a perigee pass. In the pass of figure 4 the stop mcp voltage is only turned down slightly for the last two images in the sequence when the spacecraft begins the entry to the radiation belts. The characteristic sharp drop in the O/H ratio seen midway through the previous perigee passes is not seen here.

Between the 5 July perigee passes and this date the spacecraft orbit plane has precessed to the point when the sun is again directly in the field of view of the instrument. The intense central portion of the sun pulse signal can be seen in the data from figure 4 tracking along the diamonds. At its most intense the signal from direct viewing of the sun does not swamp the perigee pass signal.

*Correlation of LENA Perigee Pass data with other indicators.* We have examined the images from 105 perigee passes made during the summer of 2000. In order to compare them with each other we use a parameter that is a measure of the total activity for each perigee pass. This parameter is the integrated flux from each image of a given perigee pass; i.e. the sum of all of the pixels in a spin-time spectrogram such as the examples shown in figures 1-4. For the most part this parameter is dominated by the perigee pass signal but can have some contributions from the sun pulse signal and radiation belt background counts.

In figure 5 we plot this integrated flux parameter for 57 perigee passes (10 June to 30 July 2000) versus the universal time the spacecraft was at perigee. What stands out clearly here is the strong diurnal variation in this parameter. Over plotted on the data is a sinusoidal function fit to those passes where the Ap index was less than or equal to 32 at the time of the pass. This function has a period of 24 hours and peaks at 0740 UT. The six points in this plot which lie furthest from this sinusoidal function have been label with the value of the Kp index at the time of the pass. The average value of Kp for the remaining 51 passes (those that cluster around the sinusoidal curve) is 3-. This figure suggests that the intensity of the perigee pass signal is a function of time of day and level of magnetic activity.

In figure 6 we have taken the data of figure 5, subtracted out the sinusoidal function, and plotted the result versus Ap. The curve fit to this data set is linear with a slop of $2.67 \times 10^7$ [flux unit/Ap unit] and a correlation coefficient of 0.74. The direct correlation between the perigee pass integrated fluxes (with diurnal variation retained) and Ap is 0.53. Removing the diurnal variation significantly improves the correlation. Clearly the total intensity of the perigee pass signal for the 10 June to 30 July 2000 data set is correlated with time of day and level of magnetic activity.

We tried this same exercise for the passes from 31 July to 29 August 2000 and got results that were somewhat different from those shown in figure 5. There was a diurnal variation with the same phase but it had smaller amplitude. This was due to the fact that on July 31, 2000 the instrument flight software was changed so that the instrument operated in a manner in which it adjusted its own sensitivity in response to changing flux levels. The effect of this change was to make the instrument more sensitive during a perigee pass and to flatten out natural variations in the intensity of the images. Analysis of the changing state of the instrument showed that during perigee passes in August 2000 the instrument sensitivity had a diurnal variation with a peak sensitivity near 2100 UT and a minimum near 0900 UT.

*What is LENA seeing in these perigee passes*? The main question before us is what is the instrument seeing in these perigee passes. Is it remotely observing some geophysical process or is it making an in situ type of measurement? To answer these questions we must first dispense with some other possible explanations for the observations. Because of the novelty of the design of this instrument and the lack of experience with these types of measurements one must ask whether or not the instrument is responding to something other than what it was intended to measure (low energy neutrals). Could it be detecting ultraviolet light or charged particles despite the fact that the instrument was designed to exclude these?

The ultraviolet light hypotheses can be dispensed with by a simple observation. In figure 4 one can see that the signal detected from looking directly at the sun is weaker that what is seen looking at the earth. The authors are unaware of any natural UV emissions from the earth that exceed those from the sun by more than an order of magnitude. In addition there is good reason to believe that much of the sun signal is solar wind neutrals *Collier et al.* [2001].

Charge particles may enter the instrument as either penetrating radiation or through the front of the instrument if they are energetic enough to get past the charged collimators. LENA sees penetrating radiation every time the spacecraft pass through the radiation belts. When this happens high fluxes are seen at all spin sectors and the whole sky "lights up". If LENA were to respond to less energetic ions or electrons that get past the deflecting collimators then the place where that would be most likely to occur would be in the auroral zone. During perigee passes from the summer of 2000 the IMAGE orbit carried the spacecraft through the southern-hemisphere auroral zone at altitudes between 1500 and 3000 km. If LENA were to detect the precipitating ions or electrons which can occur there, it should have seen them when it is looking in the zenith direction. This direction occurs at spin sector 40. From figures 1 to 4 one can see that when IMAGE is at magnetic latitudes above 65˚ there is almost nothing seen coming from the zenith direction. This is commonly the case for all of the perigee passes examined.

The other possible emission that LENA may be responding to is higher energy (>300 eV) neutrals. Analysis of the sun pulse signal by *Collier et al.* [2001] suggests that the LENA instrument can respond to high-energy (~ 2 keV) hydrogen neutrals from the solar wind as they sputter lower energy oxygen from the conversion surface. Some part of the perigee pass signal may be attributable to this emission.

What does the data itself indicate about the composition and energy of the neutrals that LENA sees in the perigee pass signal? If one takes the high stop mcp voltage data from figures 1-4 one would conclude that the dominant neutral was oxygen. The composition of the neutrals as measured by LENA cannot be taken on face value however, because of the process of sputtering. Preflight calibration measurements showed that energetic oxygen and hydrogen neutrals impacting the conversion surface could sputter hydrogen and oxygen negative ions that will be detected by the instrument. Oxygen neutrals will start sputtering $H^-$ ions at energies at least as low as 30 eV while hydrogen neutrals only start sputtering $O^-$ ions in significant numbers at energies starting at, and above, 400 eV. For example, in one test a pure 30 eV oxygen neutral input produced an oxygen to hydrogen detection ratio of one while a 30 eV hydrogen neutral input yielded a detection ratio of less than 0.1. The constancy of the O/H ratio in the perigee pass data strongly suggests that the instrument is seeing primarily one of these two neutrals, either oxygen down to at least 30 eV or hydrogen above 400 eV. The ratio then represents the sputtering yield/detection efficiency of the instrument in flight. The conversion surface is made of tungsten and it is believed that the sputtering involves water absorbed on the surface or tungsten oxides on the surface. We believe that water can be replenished onto the surface in flight as the instrument is exposed to high fluxes of thermospheric oxygen and hydrogen during orbit perigee.

The energetics of the perigee neutrals can be guessed at by some simple arguments from the data. First, the perigee pass signal is only seen near perigee. If the signal were produced by 400 eV or greater hydrogen neutrals the emissions should be visible from much further away than they are. If they were the result of low energy oxygen then they may either not have the energy to reach higher altitudes or when they do they do not have enough energy to be above the detection threshold of the instrument. Second, the lack of sharp features (as a function of spin angle) in the perigee pass signal suggests that some process is spreading out the signal that would come from a localized source like the auroral zone. Possible spreading processes are collisions, gravitational deflection and ram deflection (the shift in a neutral's apparent direction of travel due to the motion of the spacecraft). The last of these two processes are only important for oxygen neutrals below about 100 eV. Hydrogen neutrals above the energy detection threshold (above 10 eV) would not be significantly deflected by gravity or by the motion of the spacecraft.

The data strongly suggests, but does not prove, that the perigee pass signal is primarily low energy oxygen. Below the O/H cross over point [*Moore*, 1980] in the ionosphere the dominant ion is $O^+$. Energization of these ions in the auroral zone will yield low energy ions that charge exchange with thermospheric atomic oxygen to produce low energy oxygen neutrals. The high concentrations of $O^+$ and O mean that this region should be a copious producer of low energy oxygen neutrals. Add to this the various chemical processes that produce geocoronal oxygen neutrals [Hickey et al., 1995] and it is easy to see why low energy oxygen neutrals should be abundant.

**Modeling of LENA Perigee Pass Data**

What is LENA seeing in these perigee passes? As already stated the composition information strongly suggests that the main neutral is oxygen. Further more, analysis of the pattern of the signal suggests that it is low energy (< 40 eV). Where are these neutrals coming from and how are they being produced?

The near earth motion of low energy oxygen neutrals will be significantly affected by gravity, and their observation by LENA will be affected by the motion of the spacecraft. To bring these two effects into the analysis consider the following. Assume for the moment that we are dealing with an oxygen atom whose velocity vector (two dimensional) lies in the spacecraft orbit plane and has an energy *Eo* in the spacecraft frame of reference. Knowing the look direction of the instrument at each point in the spacecraft's spin, one can find the velocity vector of the atom in the spacecraft frame of reference. This vector is then transformed to a reference frame at rest with respect to the earth by adding the spacecraft's velocity vector. The energy of the atom in the earth frame is plotted in figure 7(a), in the same spin-time format as figures 1-4, for a case when *Eo* = 15 eV. As one might guess this energy has a minimum along the ram direction and a maximum at the anti-ram direction. Knowing the location of the observation point and the kinetic energy of the atom one can find if it is on an open (hyperbolic) or closed (elliptical) orbit. The same spin-time space is color-coded in figure 7(b) according to the type of orbit the observed oxygen atom is on. The perigee for each particle orbit is plotted in figure 7(c). In order to investigate the possible source locations of the oxygen we have plotted in figure 7(d) either the latitude of perigee (if it exceeds 500 km altitude) or the point in the atom's backtracked orbit where it crossed through the 500 km altitude point. Thus figure 7(d) suggests the possible latitude point of origin of the oxygen atom. Note that no latitude is plotted for hyperbolic particles on inbound trajectories.

There are several things to note about the results in figure 7. The first is the band of atoms on trapped orbits that straddles the ram direction. Although it is not apparent in figure 7 this region does not extend around the IMAGE orbit but is confined near perigee. The cause of it is simply that near perigee the spacecraft is moving fast enough so that low energy atoms, atoms whose energy is just above thermospheric values, will be visible to the instrument when it looks near the ram direction. Since these atoms have energies in the .1 to 5 eV range they can constitute part of the hot oxygen geocorona.

The second thing to note in figure 7 is that most of the atoms observed near perigee at look directions well away from ram must be on open orbits with energies above ~20 eV. As such they are unlikely to be produced by any of the chemical process responsible for hot oxygen. These atoms should be visible from farther away than the typical perigee pass signal is. There are a number of times in the LENA data set where emissions are seen coming from the direction of the earth while the spacecraft is much further away, but they are not as common as the perigee pass events shown in figures 1-4. These less common events, under current study, seem to occur most often when magnetic activity is high.

Figures 8 has the same format as figure 7 but are for oxygen atoms with *Eo* = 30 eV. One trend to note between figures 7 and 8 is the decreasing area of trapped orbits in the spacecraft frame. Above about 35 eV LENA can no longer see oxygen neutrals on trapped orbits. Also note from figure 7(d) that for spacecraft energy near 15 eV the instrument can see, while below the southern polar cap, oxygen neutrals coming from high northern latitudes.

The type of information contained in figures 7-8 can be used to illustrate how the LENA instrument would see certain source populations. Consider a source population of oxygen neutrals that originate below some geocentric distance (*Ro*) over a prescribed range of magnetic latitudes. Beyond *Ro* collisions between the oxygen neutrals and other thermospheric particles are ignored. (if *Ro* corresponds to an altitude above 1000 km this assumption is good since densities there are of order $10^5$ $cm^{-3}$ with mean free paths greater than the thermospheric oxygen scale height.) The source neutrals are assumed to have a Maxwellian distribution of energies with a specified mean energy (*To*). To build up a spin-time spectrogram showing the response of the instrument to the assumed source one must perform a double integration for each spin-time pixel. These integrations are over the polar angle (from +45˚ to –45˚ with respect to the orbit plane) and the energy response range of the instrument. The increasing effective area of the instrument with increasing energy appropriately modulates this integration. With a given spin angle, polar angle and energy the oxygen neutral's velocity in the spacecraft frame is fully specified. (Note: We are no longer using the two dimensional velocity assumption used for figures 7 and 8.) This is then transformed to the earth frame and the analysis proceeds as described above. If the backtracked orbit reaches the source region a contribution is made to the given spin-time pixel weighted by a Maxwellian factor given the particle's energy in the source region. At this point we have said nothing about the source emission strength so the resulting spin-time spectrogram is renormalized to have a peak value of near 1000 counts/sample (Or, assuming 30 eV oxygen a flux of $3.2\times10^8$ $(s\ cm^2\ sr)^{-1}$.). The main value of such an exercise is to show how a given source population can make relative contributions to different parts of the spin-time spectrogram.

Figure 9 shows an example of doing this exercise. The assumed source is a pair of auroral zones that lie between 60˚ N (60˚ S) and 75˚ N (75˚ S) magnetic latitude. The emission characteristics are assumed to be independent of MLT and confined below a geocentric distance of 1.2 $R_E$. The four panels in figure 9 show the effect of increasing the mean energy of the source oxygen neutrals from 10 to 100 eV. There are several things to note from this figure. First, in each panel there is a gap between the two branches of emissions that track across the earth. This is the result of the lack of emissions coming from the polar cap at latitudes greater than 75˚. Second, the emissions from the earth cut off on the right side because of the low latitude limit (60˚) of the source region. Third, there are oxygen neutral fluxes seen near the ram direction in all four panels but their relative contribution diminishes with increasing mean energy of the source neutrals. Fourth, strong relative fluxes are seen near the approaching limb from a considerable distance before perigee. The higher the mean energy of the source neutrals the higher the relative strength of the precursor signal compared to fluxes seen later in the pass.

In figure 10 we show four cases where the assumed source is modeled after the hot oxygen geocoronal population. The source is assumed to be uniformly distributed over the surface of the earth and lies below an altitude of about 600 km. For the lower mean energies of the source particles (1 or 2 eV) the neutral fluxes are seen in a band symmetric about the ram direction. These are particles following ballistic trajectories and are seen at points that are close to being directly over their source points. This is a prime example of ram deflection. As the mean energy of the neutrals increases the spin angle extent of the images increases with the center of the emissions shifting away from the ram direction toward the trailing limb.

**Discussion**

Based on the analysis of the LENA data and the modeling results it seems clear that the earth produces copious amounts of low energy oxygen neutrals. From the modeling results one can see that neutrals with energies below the instrument detection threshold can still be seen because of the ram effect. No doubt some of what is seen in this LENA data set is the high-energy portion of the oxygen geocorona. The tendency for the emissions to track the ram direction and the large fluxes seen around the ram could be part of this population in the 1-5 eV energy range. In addition the broad spin angle extend of the images demonstrates that higher energy neutrals must also be present. The most reasonable source for such particles is the auroral zone. The simulations demonstrate that the emissions seen spanning the earth as IMAGE approaches perigee, could be due to neutrals originating in the auroral zone. The emissions seen in the data that are the most difficult to explain are those seen between the approaching limb and the nadir after the spacecraft has passed perigee and dropped to low latitudes. They are not likely of auroral zone origin and are too energetic to be from the geocorona.

Another dilemma in the data is revealed in the modeling results. If the source populations have a sufficient range of energies to fill the extent of spin angles seen in the data then there will be particles energetic enough to be seen far from the earth. But this is not the case. The perigee pass signal is far more common than the observation by LENA of neutral fluxes coming from the earth when the spacecraft is far from the earth. How can this dilemma be resolved? One possibility is that the source is highly time-dependent, but it is difficult to believe that the source always waits for the spacecraft to arrive at perigee before turning on. Another possibility is that the model is not restrictive enough in terms of the MLT extent or pitch angle distribution of the source population. This idea has not yet been tested. It has been suggested that scattering in the LENA collimator (particle reflection from a surface in the entrance collimator that changes the apparent arrival direction) could broaden the apparent angular extent of a source and thus eliminate the need for higher energy particles. Assume that the main signal is a 1-2 eV hot oxygen geocoronal population and that its broad spin angle extent is due to scattering. This signal will appear near the earth but it will be centered on the ram direction. The data shows significantly broader spin distributions of fluxes than are seen in figure 10 but they are not centered on the ram so higher energy particles must be present.

One result illustrated by figure 9 is that a neutral source restricted to a small region of the earth's surface (such as the auroral zone) cannot fully account for the emission patterns seen in the data. The broad pattern of emissions suggests those oxygen neutrals with energies greater than 10 eV must originate over fairly broad regions of the earth. How then do we get neutrals with auroral zone energies to appear to come from regions outside the auroral zone? Neutral-neutral collisions are one possible way to spread out the apparent size of the source region. Energetic neutrals created at low enough altitude in the auroral zone may experience several collisions before they escape the earth. Energetic neutrals created at intermediate altitudes (700-2000 km) may dip down into the lower atmosphere where they can experience collisions that, in some cases, deflect them outward far from their point of creation.

The diurnal variation in total perigee pass intensities as displayed in figure 5 is an important clue as to where these particles are coming from. One way to explain this variation is to assume that the dayside auroral zone is the main source of the oxygen neutrals and that the strength of the source increases when the auroral zone is most sunward. During the month of June the southern polar cap is in winter and does not receive direct sunlight. According to the MSIS model [*Hedin*, 1987], a position that is at 1200 MLT and $-80^{\circ}$ magnetic latitude will experience about a factor of 5 variation in the local abundance of atomic oxygen over the course of a day. The highest value will occur at about 0500 UT and the minimum at about 1700 UT. This is close to the same basic trend as the data, in terms of the timing of the peak and minimum intensities. The diurnal variation may represent a variation in the original ion population, the neutral population with which it charge exchanges, or both. We are unaware, however, of any reports of a diurnal variation in the total ion outflow flux.

There is evidence in the spin angle extent of the perigee pass images that the source of the neutrals covers a range of energies from near thermal to as much as 100 eV. Another pattern seen in the perigee passes is the tendency for the high latitude images to vary more abruptly than the low latitude images. By that we mean in the 4-6 images taken pre perigee, when the spacecraft is at high southern magnetic latitudes, there is a tendency for more abrupt and frequent changes in intensities and spin angular extents of the fluxes. The 4-7 images taken after these show much less variability or a much smoother variation from one image to the next. This trend is particularly apparent in the late July and August 2000 data. One interpretation of this is that the two sets represent two different particle populations or different source regions.

In their analysis of IMAGE (and LENA) data *Fuselier et al.* [2001] describe an ion outflow event that appears to have been triggered by the arrival of an interplanetary shock at the earth. On June 8, 2000 at about 0912 UT a shock, with about a factor of 10 increase in ram pressure, collided with the magnetosphere. At this time a response is seen in the ionosphere with an increase in proton auroral emissions near local noon and an increase in the flux of low energy neutrals seen coming from the earth. About 37 minutes later LENA sees a much larger increase in the flux of neutrals coming from the earth. Given IMAGE's distance from the earth the delay time is consistent with the travel time for 30 eV oxygen neutrals. Although the timing of the second neutral burst may be coincidental the proposed scenario of *Fuselier et al*. [2001] is consistent with one of our main conclusions. That is that most of the neutrals produced near the earth are low energy oxygen.

**Summary**

Although a full understanding of the perigee pass signal has not been achieved there are some clear aspects. Part of the signal, the part clustered around the ram, is very likely part of the hot oxygen geocorona. These atoms are on ballistic trajectories and are produced in many regions (not just the auroral zone) by a variety of ionospheric chemical reactions [*Hickey et al.*, 1995]. As the look direction moves away from ram one is seeing more energetic atoms, which must be produced by other processes. One of these is ion energization in the auroral zone followed by charge exchange with thermospheric atomic oxygen. Another possibility is the creation of oxygen backsplash by precipitating oxygen ions from the ring current or plasma sheet [*Ishimoto et al.*, 1992]. The LENA data suggest that some process must be acting to expand the apparent source region of these more energetic neutrals beyond the size of a typical auroral zone. Energetic neutrals created at low enough altitude may experience several collisions before they escape the earth. Energetic neutrals created at intermediate altitudes (700-2000 km) may dip down into the lower atmosphere, at points well away from their origin, where they can experience collisions that deflect them outward.

Our main conclusions are:

1. There is always present in the near earth environment measurable fluxes of low energy ($< 50$ eV) neutral oxygen atoms.
2. Evidence suggests at least two main sources for these particles. One tends to be highly variable producing more energetic particles ($> 20$ eV) and the other tends to be less variable producing lower energy particles ($< 20$ eV), assuming neutrals are oxygen.
3. The neutral production rate increases with increasing magnetic activity.
4. During southern-hemisphere winter the overall neutral production rate varies diurnally with its peak near 0740 UT and minimum near 1940 UT.
5. Near perigee neutral fluxes are seen coming from a broad range of directions so that a localized source, such as the auroral zone, alone can't produce it.
6. Gravitational and ram deflection alone cannot account for the diffuse images seen at perigee.

*Acknowledgements.* The authors thank the NASA MidEx program for making the IMAGE mission possible and to the IMAGE/LENA team for providing the data and helping with its interpretation. The work at Mission Research Corporation was supported by an IMAGE mission subcontract (NAS8-98203) from the Marshall Space Flight Center.

**References**

André, M., and A. Yau, Theories and observations of ion energization and outflow in the high latitude magnetosphere, *Space Sci. Rev.*, *80*, 27, 1997.

C:son Brandt, P., S. Barabash, E. C. Roelof, and C. J. Chase, Energetic neutral atom imaging at low altitude from the Swedish microsatellite Astrid: Observations at low (≤10 keV) energies, *J. Geophys. Res.*, *106*, 24663, 2001.

C:son Brandt, P., S. Barabash, G. R. Wilson, E. C. Roelof, and C. J. Chase, Energetic neutral atom (ENA) imaging at low (≤10 keV) energies from Astrid: Observations and simulations, *J. Atm. Solar-Terr. Phys.*, *62*, 901, 2000.

Collier, M. R., et al., Observations of neutral atoms from the solar wind, *J. Geophys. Res.*, *106*, 24893, 2001.

Fuselier, S. A., et al., Ion outflow observed by IMAGE: Implications for source region and heating mechanism, *Geophys. Res. Lett.*, *28*, 1163, 2001.

Hedin, A. E., MSIS-86 Thermospheric Model, *J. Geophys. Res.*, *92*, 4649, 1987.

Henderson, M. G., G. D. Reeves, H. E. Spence, R. B. Sheldon, A. M. Jorgensen, J. D. Blake, and J. F. Fennell, First energetic neutral atom images from Polar, *Geophys. Res. Lett.*, *24*, 1167, 1997.

Herrero F., and M. F. Smith, Imager of low-energy neutral atoms (ILENA): Imaging neutrals from the magnetosphere at energies below 20 keV, SPIE, vol. 1744, 32, 1992.

Hickey, M. P., P. G. Richards, and D. G. Torr, New sources for the hot oxygen geocorona: Solar cycle, seasonal, latitudinal, and diurnal variations, *J. Geophys. Res.*, *100*, 17377, 1995.

Ishimoto, M., G. R. Romick and C.-I. Meng, Energy distribution of energetic $O^+$ precipitation into the atmosphere, *J. Geophys. Res.*, *97*, 8619, 1992.

Jorgensen, A. M., H. E. Spence, M. G. Henderson, G. D. Reeves, M. Suguira, and T. Kamei, Global energetic neutral atom (ENA) measurements and their association with the Dst index, *Geophys. Res. Lett.*, *24*, 3173, 2001.

Lynch, K. A., R. L. Arnoldy, P. M. Kintner, and J. Bonnell, The AMICIST auroral sounding rocket: A comparison of transverse ion acceleration mechanisms, *Geophys. Res. Lett.*, *23*, 3293, 1996.

Moore, T. E., Modulation of terrestrial ion escape flux by low-altitude acceleration and charge exchange chemistry, *J. Geophys. Res.*, *85*, 2011, 1980.

Moore, T. E., et al., The low energy neutral atom imager for IMAGE, in *The IMAGE Mission*, edt. J. L. Burch, Kluwer Academic Publ., Dordrecht, The Netherlands, 2000.

Moore, T. E., et al., Low energy neutral atoms in the magnetosphere, *Geophys. Res. Lett.*, *28*, 1143, 2001.

Moore, Thomas E., Michael R. Collier, Mei-Ching Fok, Stephen A. Fuselier, David G. Simpson, Peter Wurz, Interstellar atom and neutral solar wind observations from IMAGE, *Eos Trans. AGU*, 83(19), Spring Meet. Suppl., Abstract SH32C-01, 2002.

Reeves, G. D., and M. G. Henderson, The storm-substorm relationship: Ion injection in geosynchronous measurements and composite energetic neutral atom images, *J. Geophys. Res*., *106*, 5833, 2001.

Roelof, E. C., Energetic neutral atom image of a storm-time ring current, *Geophys. Res. Lett.*, *14*, 652, 1987.

Yau, A. W., P. H. Beckwith, W. K. Peterson, and E. G. Shelley, Long-term (solar cycle) and seasonal variations of upflowing ionospheric ion events at DE1 altitudes, *J. Geophys. Res*., **90**, 6395, 1985.

Yau, A., and M. André, Source of ion outflow in the high latitude ionosphere, *Space Sci. Rev.*, *80*, 1, 1997.

## Figure Captions

**Figure 1.** LENA data from the first perigee pass of June 15, 2000. Each vertical band in the spin-time spectrogram is a set of images collapsed over polar angle mass and energy. Counts in the spin time spectrogram are for valid hydrogen and oxygen events, corrected for background. The dotted line indicates the nadir direction. The upper (lower) dot-dashed line indicates the trailing (approaching) limb. The dashed line indicates the ram direction. Pixels marked with a diamond indicate the spin phase when the LENA look direction is closest to the sun. Counts were converted to flux levels by assuming that the neutrals were oxygen with an energy of 30 eV. (Higher energies or a larger hydrogen component would reduce these fluxes.) The O/H plot below the spectrogram gives the ratio of the number of background corrected valid O events to H events for the entire image.

**Figure 2.** Same as figure 1 but for the first perigee pass of July 5, 2000.

**Figure 3.** Same as figure 1 but for the second perigee pass of July 5, 2000.

**Figure 4.** Same as figure 1 but for the second perigee pass of August 24, 2000.

**Figure 5.** Plot of the total number of valid O and H events for each perigee pass between 10 June and 30 July 2000. The most intense points are labeled with the value of Kp at the time of the pass. The sinusoidal curve was obtained by a least squares fit to all of the passes for which the concurrent value of the Ap index was less than or equal to 32 (Kp = 4+).

**Figure 6.** Same points that are plotted in figure 5 but now plotted versus Ap. The sinusoidal variation noted in figure 5 has been removed from these data. The correlation coefficient between the corrected total counts and Ap is 0.74.

**Figure 7.** In the analysis for this figure oxygen neutrals are assumed to have velocity vectors that lie in the spacecraft orbit plane and have energy $Eo$ of 15 eV in the instrument frame of reference. The spacecraft ephemeris used for this analysis is that of the first perigee pass of July 5, 2000. (a) The energy of the oxygen neutrals after spacecraft ram effects are subtracted. (b) Type of orbit (elliptical or hyperbolic) for the neutral and whether or not the radial component of its velocity is positive (outbound) or negative (inbound). (c) Perigee of the orbit the neutral is on. (d) For the backtracked orbit, the latitude at which perigee or 500 km altitude is reached, depending on which is first.

**Figure 8.** Same as figure 10 but for a value of $Eo$ = 30 eV.

**Figure 9.** Simulated spin-time spectrograms for a hypothetical auroral zone source that lies between 60˚ and 75˚ magnetic latitude. The emitted neutrals are assumed to be oxygen with a Maxwellian distribution of energies in a source region that lies below a geocentric distance of 1.2 $R_E$ (altitude of 1274 km). The spacecraft ephemeris used for this analysis is that of the first perigee pass of July 5, 2000. The four panels show the effect of varying the temperature of the source population from 10 to 100 eV. The LENA oxygen low energy cutoff was assumed to be 10 eV. The effects of gravitational and ram deflection, based on the analysis of figures 7-8, are included here.

**Figure 10.** Same as figure 9 but for a hypothetical hot oxygen source that covers the entire earth below an altitude of 637 km (geocentric distance of 1.1 $R_E$).

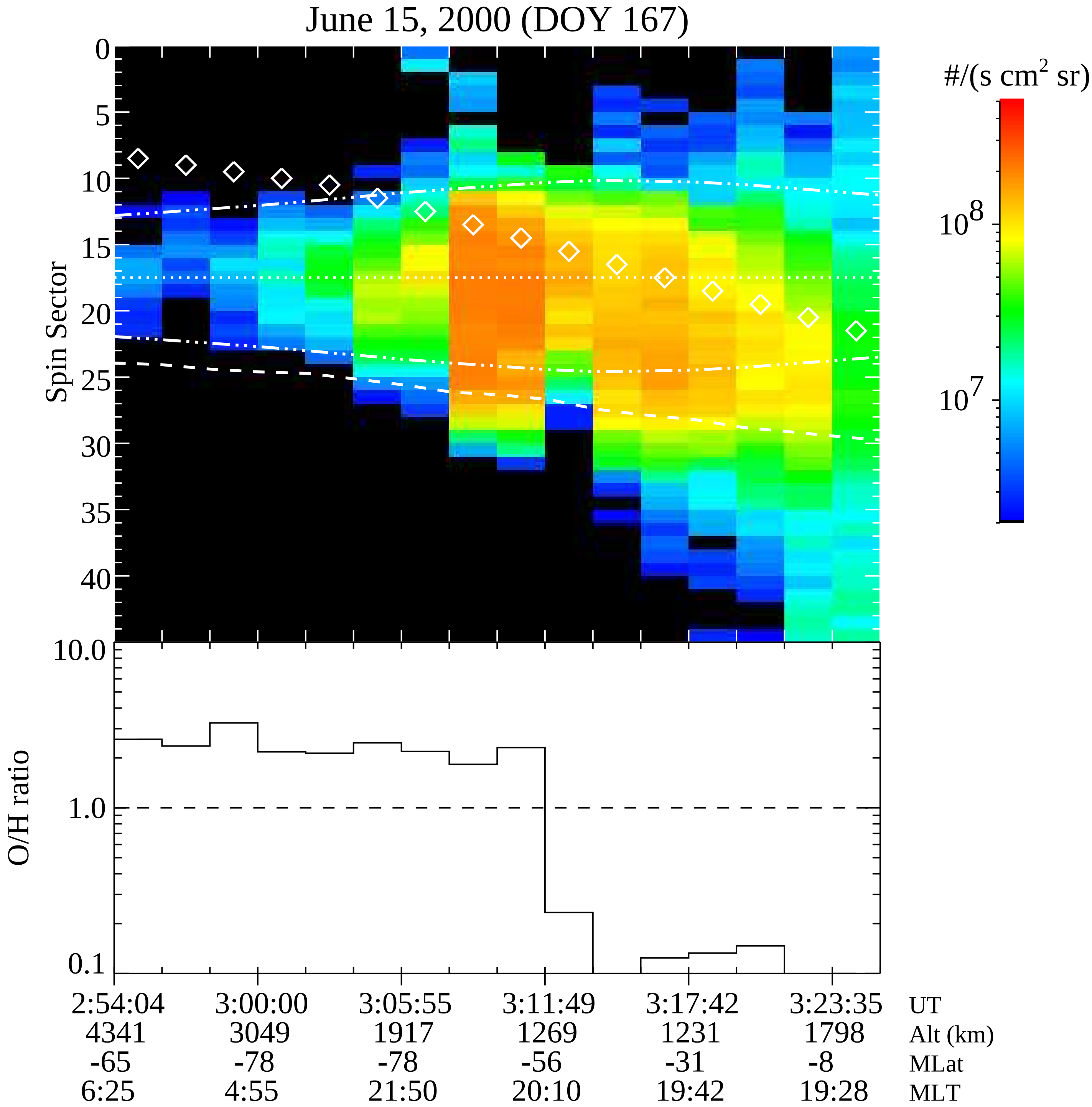

June 15, 2000 (DOY 167)
Spin Sector
0
5
10
15
20
25
30
35
40
#/(s cm$^2$ sr)
$10^8$
$10^7$
O/H ratio
10.0
1.0
0.1
2:54:04 3:00:00 3:05:55 3:11:49 3:17:42 3:23:35 UT
4341 3049 1917 1269 1231 1798 Alt (km)
-65 -78 -78 -56 -31 -8 MLat
6:25 4:55 21:50 20:10 19:42 19:28 MLT

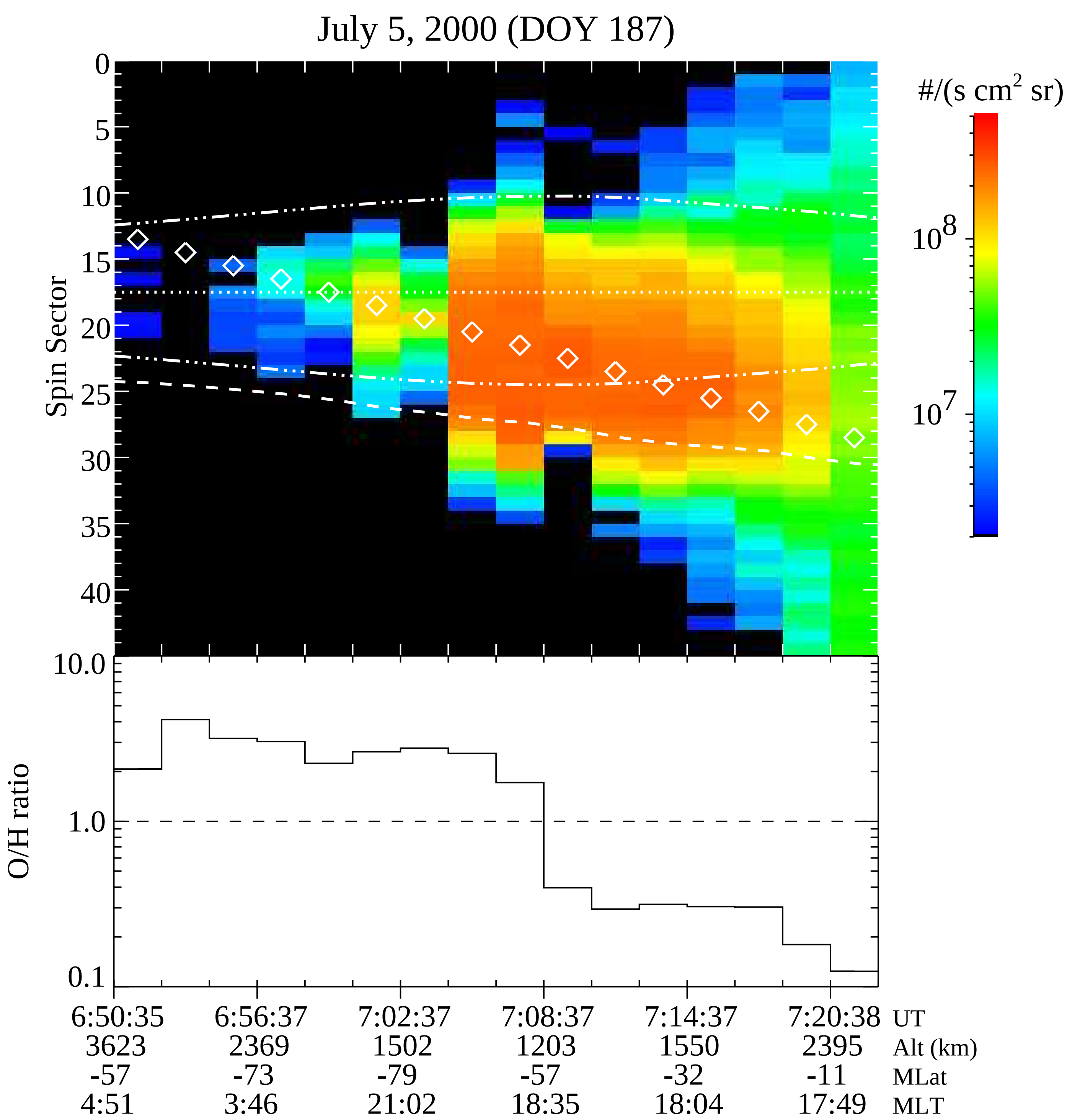

July 5, 2000 (DOY 187)
Spin Sector
#/(s cm$^2$ sr)
$10^8$
$10^7$
O/H ratio
10.0
1.0
0.1
0
5
10
15
20
25
30
35
40
6:50:35 6:56:37 7:02:37 7:08:37 7:14:37 7:20:38 UT
3623 2369 1502 1203 1550 2395 Alt (km)
-57 -73 -79 -57 -32 -11 MLat
4:51 3:46 21:02 18:35 18:04 17:49 MLT

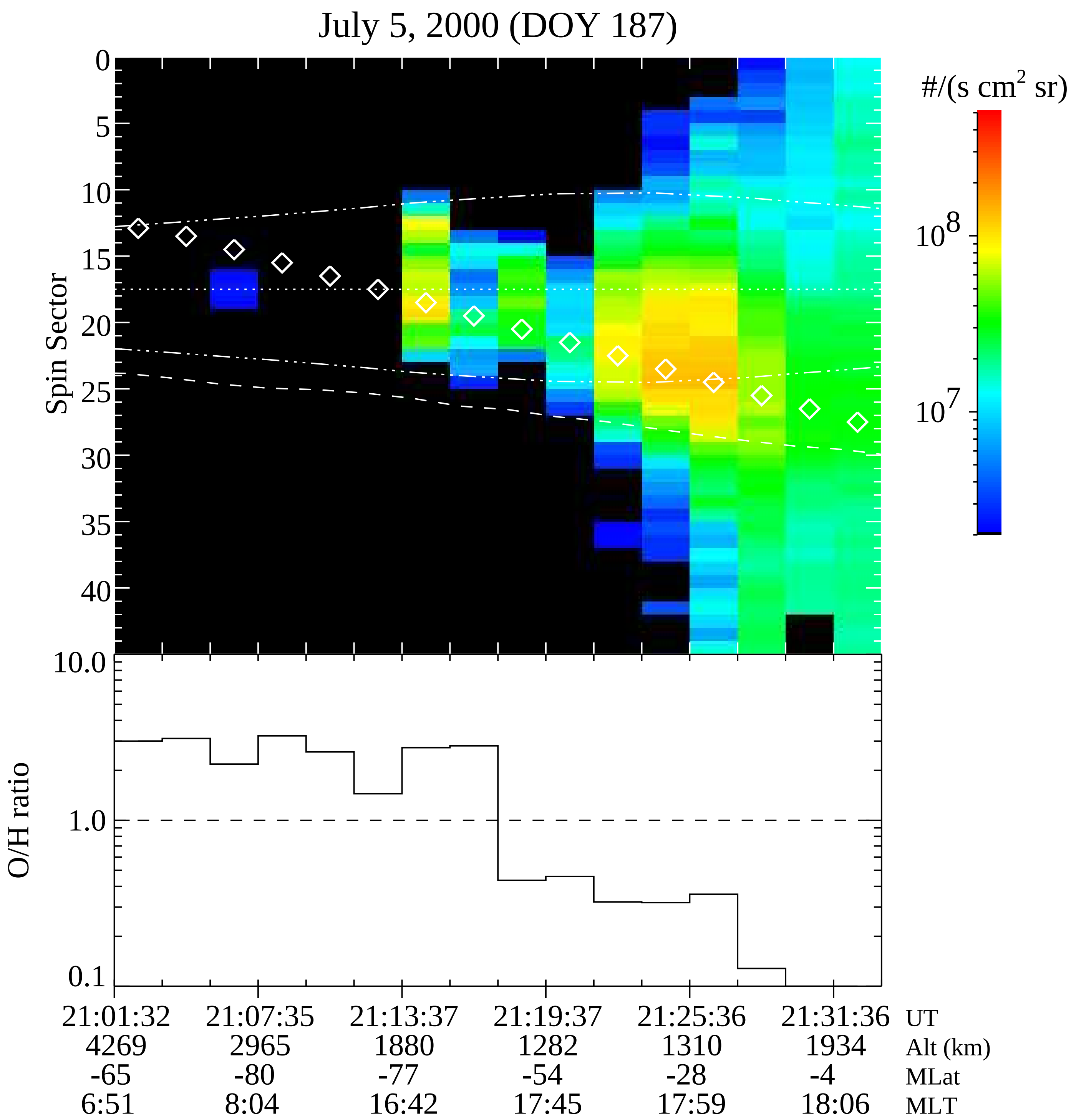
July 5, 2000 (DOY 187)
Spin Sector
#/(s cm$^2$ sr)
$10^8$
$10^7$
O/H ratio
10.0
1.0
0.1
0
5
10
15
20
25
30
35
40
21:01:32
4269
-65
6:51
21:07:35
2965
-80
8:04
21:13:37
1880
-77
16:42
21:19:37
1282
-54
17:45
21:25:36
1310
-28
17:59
21:31:36
1934
-4
18:06
UT
Alt (km)
MLat
MLT

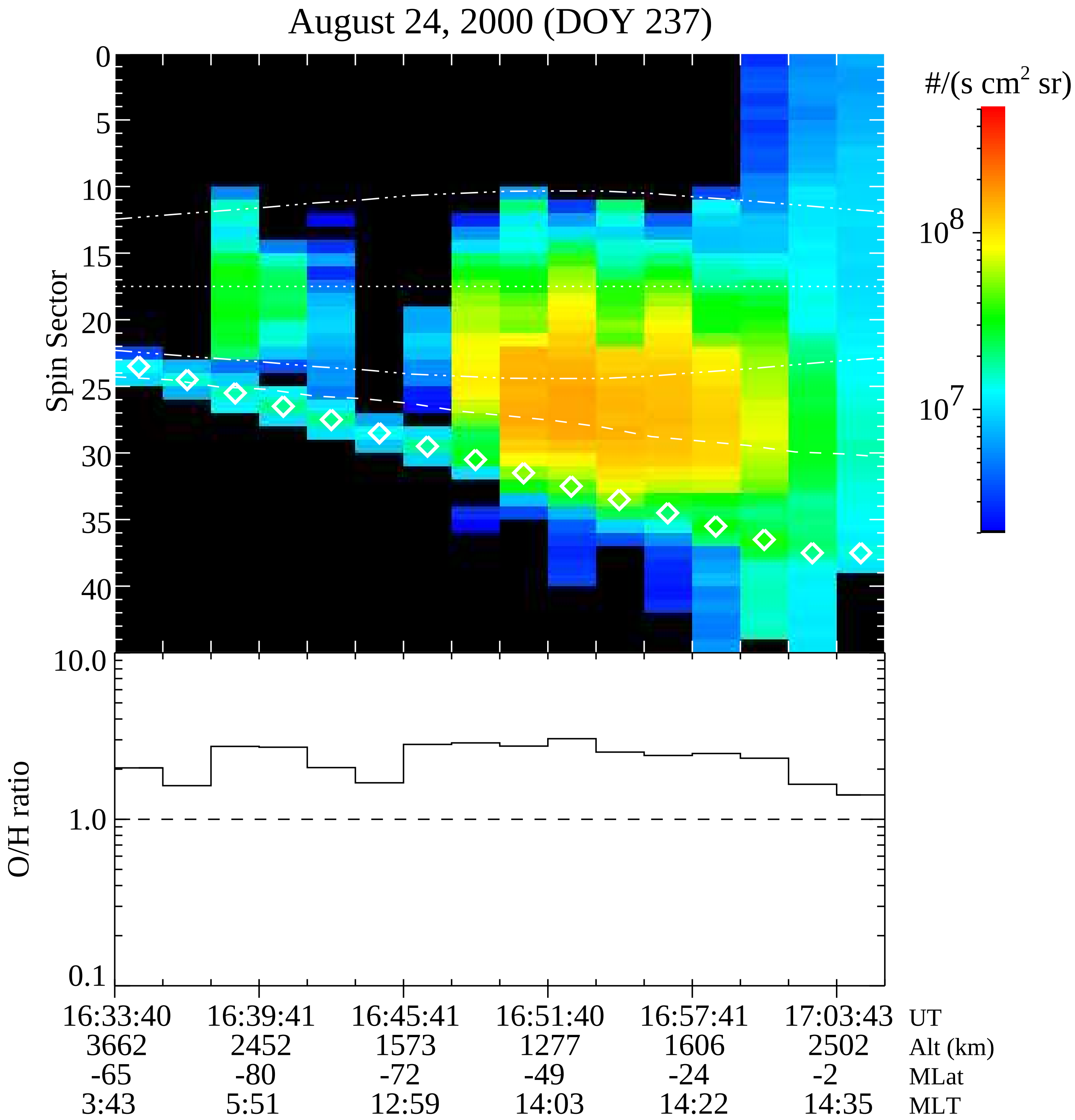
August 24, 2000 (DOY 237)
Spin Sector
#/(s cm² sr)
O/H ratio
UT
Alt (km)
MLat
MLT
16:33:40 3662 -65 3:43
16:39:41 2452 -80 5:51
16:45:41 1573 -72 12:59
16:51:40 1277 -49 14:03
16:57:41 1606 -24 14:22
17:03:43 2502 -2 14:35

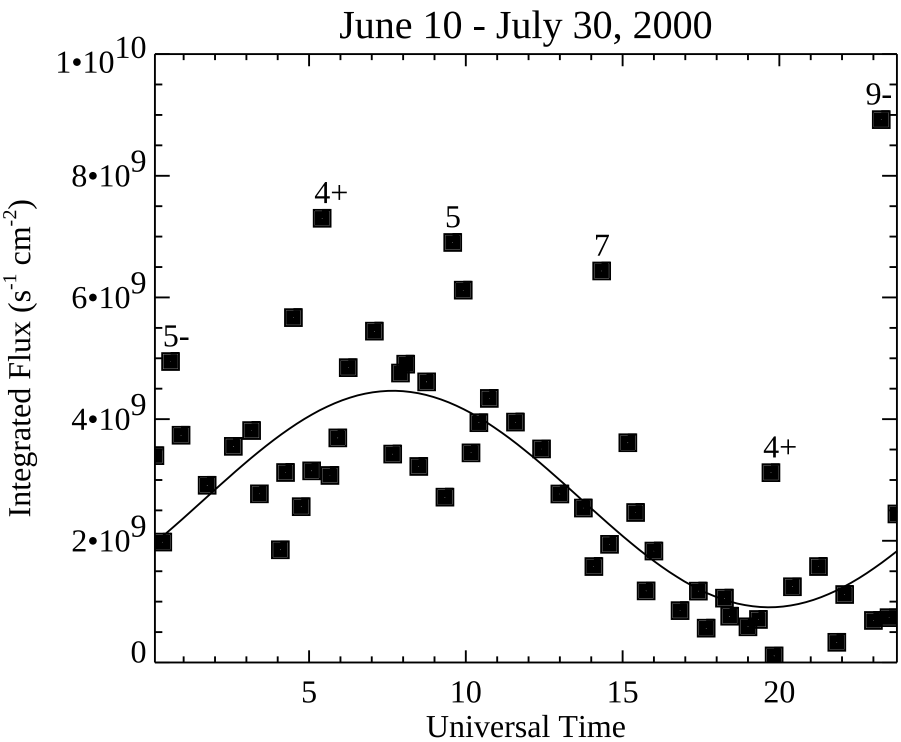

June 10 - July 30, 2000
Integrated Flux ($s^{-1}$ $cm^{-2}$)
$1•10^{10}$
$8•10^9$
$6•10^9$
$4•10^9$
$2•10^9$
0
5-
4+
5
7
4+
9-
5
10
15
20
Universal Time

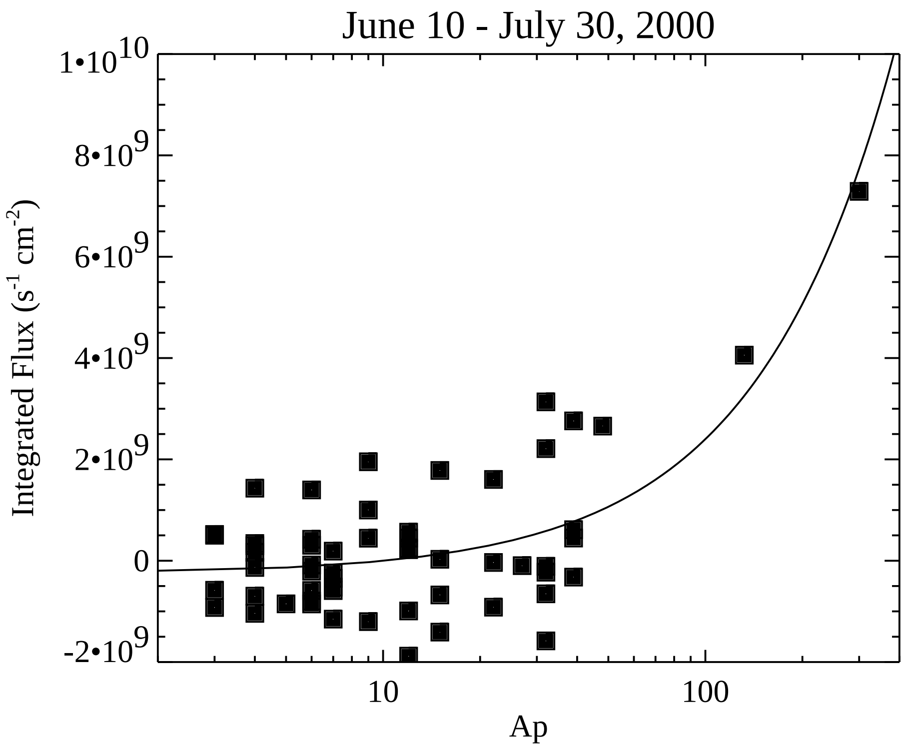

June 10 - July 30, 2000
1•10^10
8•10^9
6•10^9
4•10^9
2•10^9
0
-2•10^9
Integrated Flux (s^-1 cm^-2)
10
100
Ap

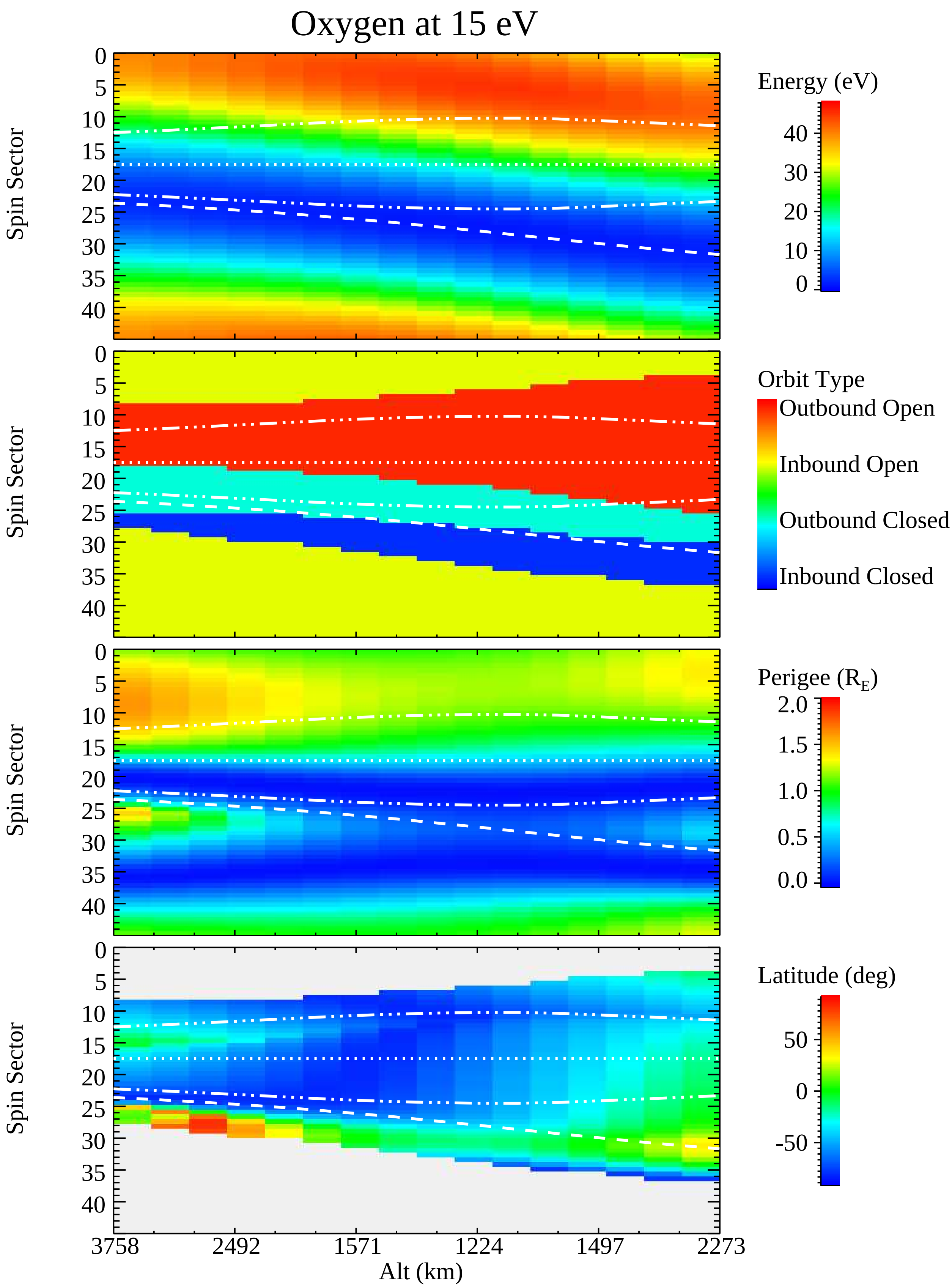
Oxygen at 15 eV
Spin Sector
Energy (eV)
Orbit Type
Outbound Open
Inbound Open
Outbound Closed
Inbound Closed
Perigee ($R_E$)
Latitude (deg)
3758
2492
1571
1224
1497
2273
Alt (km)

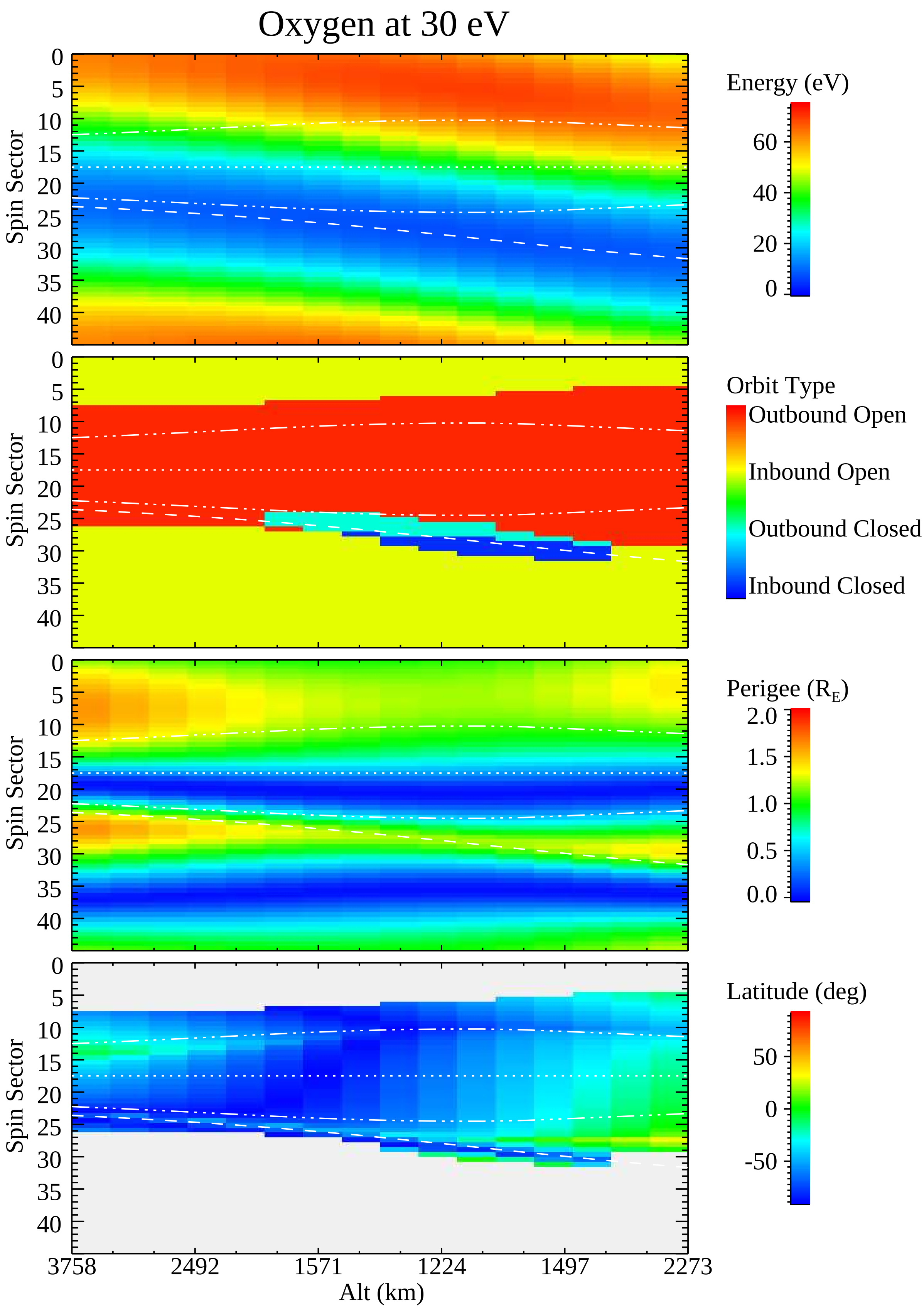
Oxygen at 30 eV
Spin Sector
Energy (eV)
Orbit Type
Outbound Open
Inbound Open
Outbound Closed
Inbound Closed
Perigee ($R_E$)
Latitude (deg)
3758
2492
1571
1224
1497
2273
Alt (km)

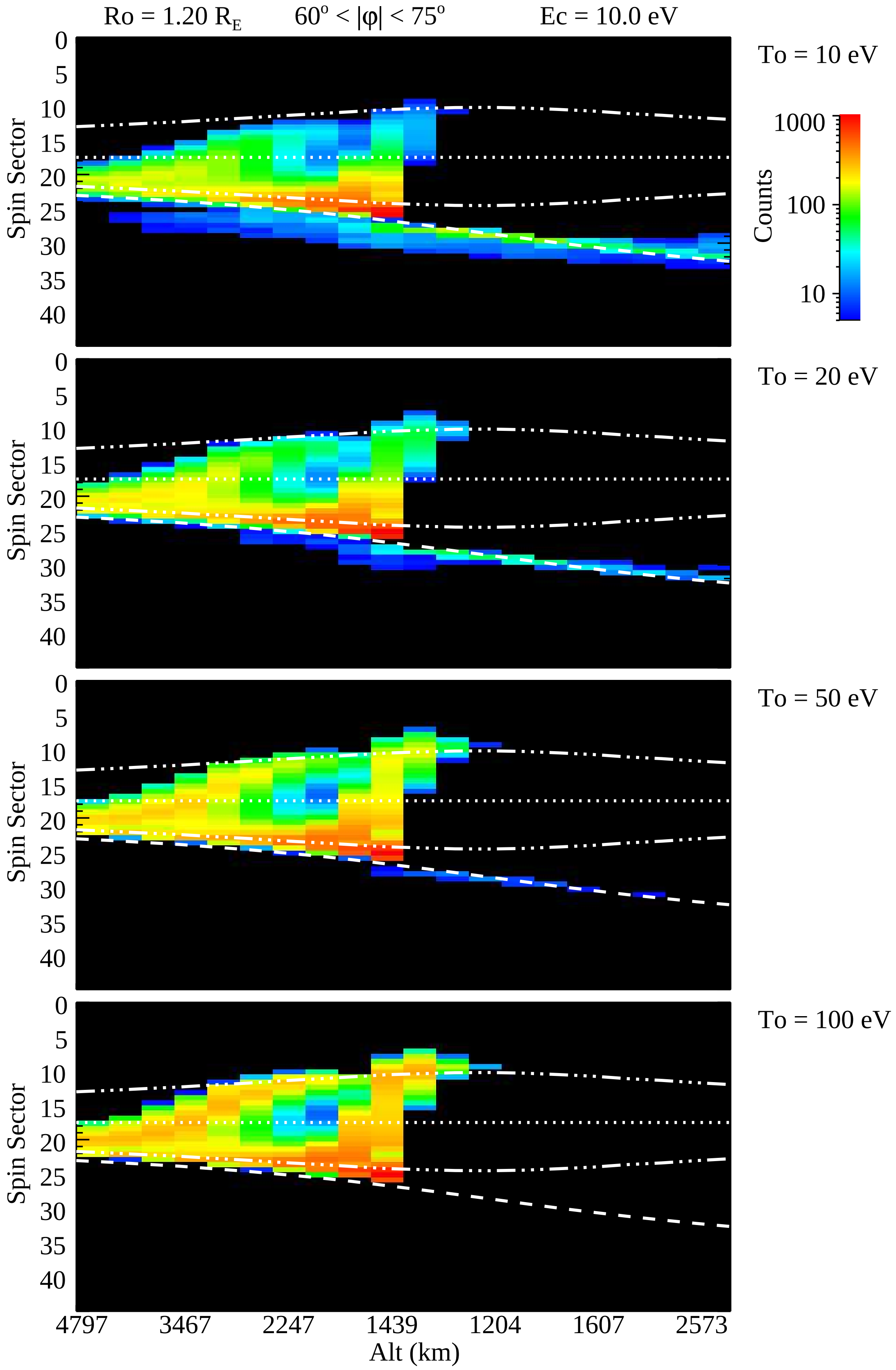

Ro = 1.20 R_E
60° < |φ| < 75°
Ec = 10.0 eV
To = 10 eV
To = 20 eV
To = 50 eV
To = 100 eV
Spin Sector
Counts
1000
100
10
0
5
10
15
20
25
30
35
40
4797
3467
2247
1439
1204
1607
2573
Alt (km)

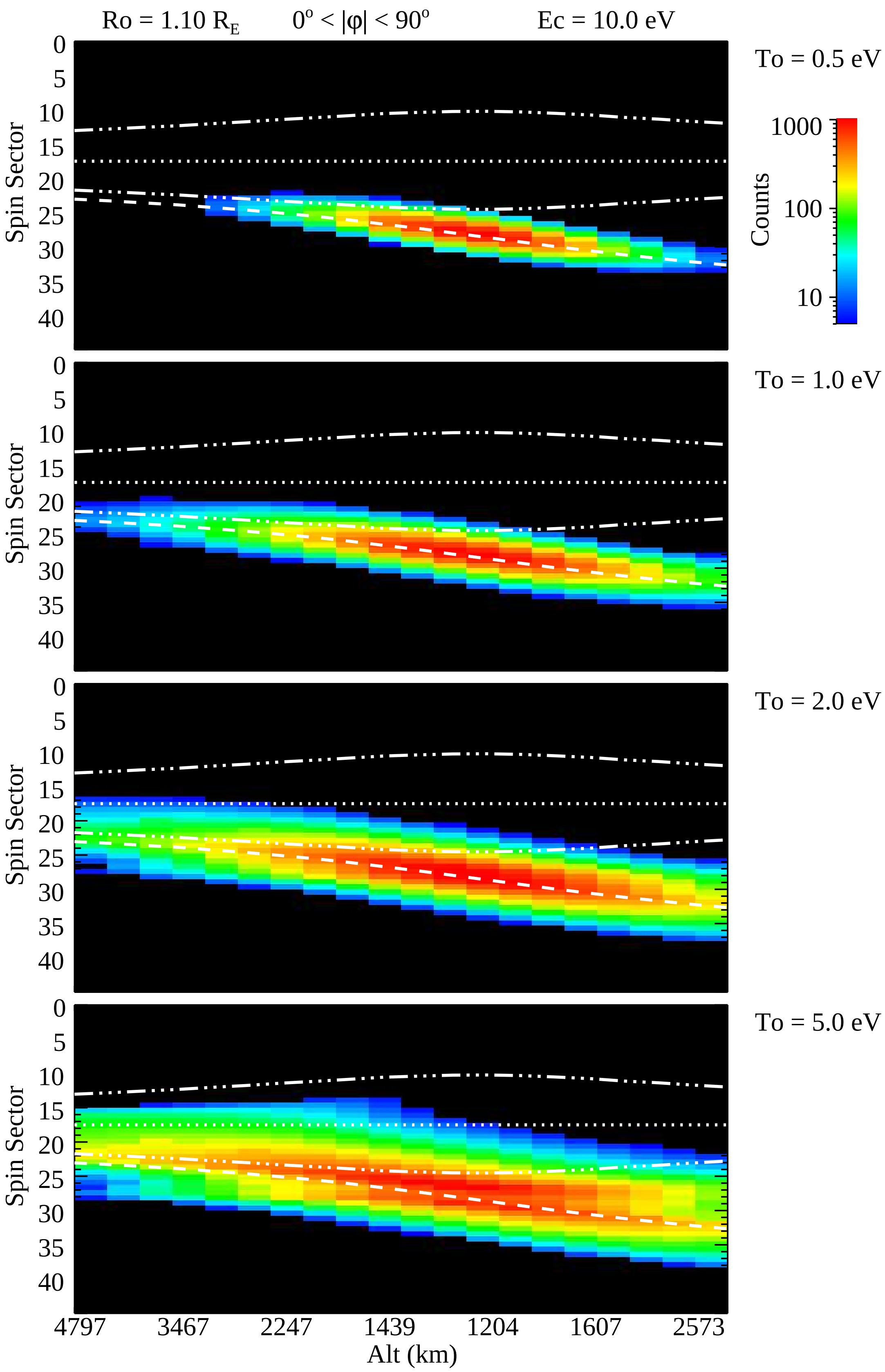

Ro = 1.10 $R_E$
$0^o < |\varphi| < 90^o$
Ec = 10.0 eV
To = 0.5 eV
To = 1.0 eV
To = 2.0 eV
To = 5.0 eV
Counts
1000
100
10
Spin Sector
0
5
10
15
20
25
30
35
40
4797
3467
2247
1439
1204
1607
2573
Alt (km)